

Hepatic Fatty Acid–Binding Proteins of a Teleost, *Lateolabrax japonicus*. The Primary Structures and Location of a Disulfide Bond¹

Shoji Odani,^{*2} Katsuya Baba,^{*} Yutaka Tsuchida,^{*} Yutaka Aoyagi,[†] Shuji Wakui,[‡] and Yoshiaki Takahashi[§]

^{*}Department of Biology, Faculty of Science, Niigata University, Ikarashi, Niigata 950-2181; [†]Department of Internal Medicine III, School of Medicine, Faculty of Medicine, Niigata University, Asahimachi, Niigata 951-8122;

[‡]Department of Physiology, School of Medicine, Faculty of Medicine, Niigata University, Asahimachi, Niigata 951-8122; and [§]Department of Medical Technology, School of Health Science, Faculty of Medicine, Niigata University, Asahimachi, Niigata 951-8122

Received September 6, 2000; accepted October 24, 2000

Two fatty acid–binding proteins (FABP), FABP-1 and FABP-2, were purified from the liver cytosol of the teleost, *Lateolabrax japonicus* (Japan sea bass), and characterized. The complete primary structure of FABP-2 was determined by protein analysis to be the following: MDFSGTWQVY AQENYEEFLR AMELPADVIK MAKDIKPITE IKQSGNDFVV TSKTPGKTVT NSFTIGKEAD ITTMDGKKIR CVVNLEGGKL VCNTGKFCCHI QELRGEMVE TLTMGSTTLI RKSCKM. Partial peptide sequences of FABP-1 were also determined. Phylogenetic analysis indicates that FABP-2 is a homologue of mammalian hepatic FABP, whereas FABP-1 is most similar to the members of mammalian cardiac FABP subfamily. *L. japonicus* FABP-2 contains three cysteine residues, and a disulfide bond is identified between Cys-81 and Cys-92. A theoretical model of FABP-2 generated by a homology modeling method indicates close proximity of the two cysteine residues in the three-dimensional structure. This is a rather rare case of cytosolic protein having a disulfide bond under the normally reducing conditions of the cytosol, though the presence or absence of disulfide bonds does not seem to affect the ligand-binding ability.

Key words: amino acid sequence, disulfide bond, fatty acid–binding protein, fish, *Lateolabrax japonicus*.

Fatty acid–binding proteins (FABPs) or intracellular lipid-binding proteins constitute a large family of tissue-specific proteins with affinities for long-chain fatty acids and/or other hydrophobic molecules. Fourteen members of this family have so far been recognized in mammals, and these are usually grouped into the four major subfamilies of cardiac, hepatic, and intestinal FABPs and retinoid-binding proteins by the phylogenetic analysis (1, 2). Although FABPs from non-mammalian vertebrates have been far less extensively studied, recent reports showed interesting tissue distributions of FABPs in lower vertebrates, especially in fish. For example, nurse shark (*Ginglymostoma cirratum*) and lamprey (*Entosphenus japonicus*) livers contain cardiac FABP instead of hepatic FABP (3, 4), and the liver of another shark, *Halaetunus bivius*, expresses both cardiac and hepatic FABPs (5). While a single hepatic FABP is expressed in mammalian liver, as many as five different FABPs appear to be present in the liver of elephant fish (*Callorhynchus callorhynchus*) (6). These reports suggest some unique aspect of fatty acid (lipid) metabolism

and function of the fish livers. We investigated the liver FABP in a typical bony fish, *Lateolabrax japonicus* (Japan sea bass), and isolated two FABPs, one of which was closely related to the mammalian hepatic FABP and the other to the members of cardiac FABP subtype. Recently we have identified disulfide bonds in rat cutaneous FABP despite its cytosolic origin (7). Interestingly, we have also found that one of the sea bass hepatic FABPs contains a disulfide bond, and in this report, we describe isolation, characterization, and primary structure of liver FABPs of *L. japonicus* as well as location of a disulfide bond, which is supported by a molecular model building study.

MATERIALS AND METHODS

Materials—*L. japonicus* adults (70–90 cm in total length and 2–3 kg in body weight) were caught on the coast of the Sea of Japan near Niigata. Chromatographic materials were products of Pharmacia, Uppsala, (Sephadex, Sephacryl, and Superdex), Tosoh, Tokyo (ODS-120T columns), Shiseido, Tokyo (Capcell Pak C8 and C18 columns), and Sigma-Aldrich Japan, Tokyo (Lipidex 1000). Lysyl endopeptidase from *Achromobacter lyticus* and *Staphylococcus aureus* V8 protease were purchased from Wako Pure Chemicals, Osaka. Acylamino acid–releasing enzyme from porcine liver was obtained from Takara Shuzo, Kyoto. Reagents for amino acid sequence analysis were from Perkin-Elmer Japan, Yasuura. Anhydrous hydrazine was obtained from Pierce Chemical, Rockford. 11-[(5-Dimethylamino-

¹ This research was supported by a Grant-in-Aid for Scientific Research (C-10680579) from the Ministry of Education, Science, Sports and Culture of Japan.

² To whom correspondence should be addressed. Tel: +81-25-262-6174, Fax: +81-25-262-6116, E-mail: sodani@sc.niigata-u.ac.jp
Abbreviations: FABP, fatty acid-binding protein; DAUDA, 11-[(5-dimethylamino)naphthalene-1-sulfonyl]amino]undecanoic acid.

naphthalene-1-sulfonyl)amino]undecanoic acid (DAUDA) and *cis*-parinaric acid were products of Molecular Probes, Eugene.

Purification of Sea Bass Liver FABP—The livers (50 g) of sea bass were minced and homogenized with 100 ml of 0.1 M Tris-HCl, pH 8.0, 0.25 M sucrose, and 1 mM EDTA. The homogenate was centrifuged for 90 min at 100,000 $\times g$, and the supernatant was condensed to 15 ml by ultrafiltration using an Amicon YM-10 membrane (Millipore, Bedford). The sample was then subjected to gel filtration on a Sephadex G-75 column (5 \times 100 cm) equilibrated with 10 mM Tris-HCl, pH 8.5. Fractions containing proteins with molecular mass of approximately 15,000 Da as determined by SDS-PAGE were pooled, condensed by ultrafiltration, and subjected to a second gel filtration on a Sephacryl S-100 column (3 \times 100 cm) equilibrated with 30 mM Tris-HCl, pH 8.6, 1 mM EDTA. The low-molecular-mass proteins in the Sephacryl S-100 fractions were again detected by SDS-PAGE, and individual fractions containing low-molecular-mass proteins were examined for protein profiles by HPLC on an octylsilane column (Capcell Pak C8, 4.6 \times 150 mm) equilibrated with 0.05% trifluoroacetic acid containing 1% acetonitrile. A linear 40-min gradient of 1–75% acetonitrile concentration in 0.05% trifluoroacetic acid was used for elution. The flow rate was 1.0 ml/min. Proteins were detected by measuring the absorbance at 215 nm. Fractions containing pure proteins were pooled separately.

Reduction and S-Alkylation of Sea Bass Liver FABPs—FABP-2 (80 nmol) was reduced with 10 mM dithiothreitol in 300 μ l of 6 M guanidine-HCl in 1 M Tris-HCl buffer, pH 8.0, containing 5 mM EDTA for 3 h at 55°C. Cysteine thiol groups were alkylated by incubation with 20 mM iodoacetic acid for 20 min in the dark at 25°C. The reagents were removed by ultrafiltration using an Amicon YM10 Centriprep filter device (Millipore, Bedford).

Enzymatic Digestion and Separation of Peptides—The reduced, S-alkylated sea bass protein (33 nmol) was digested overnight with 10 μ g of *Achromobacter* lysyl endopeptidase (8) at room temperature in 10 mM Tris-HCl buffer, pH 8.5, containing 2 M guanidine-HCl. An aliquot of the digest corresponding to 7 nmol of the protein was separated on an octadecylsilane column (4.6 \times 250 mm, ODS-120T) equilibrated with 1% acetonitrile in 0.05% trifluoroacetic acid. The acetonitrile concentration was increased linearly from 1% to 75% in 135 min. The flow rate was 0.5 ml/min. Peptides were detected by the absorbance at 215 nm. Peak fractions were checked for purity by rechromatography on the same column using a different solvent system of 10 mM ammonium formate, pH 4.5, instead of 0.05% trifluoroacetic acid. The protein was also digested with *Staphylococcus aureus* V8 protease (1:36, w/w) in 50 mM ammonium acetate, pH 4.0, for 5 h at 37°C, and peptides were separated in the same fashion.

Removal of the N-Terminal Blocking Group—An N-terminal lysyl endopeptidase peptide (1 nmol) with blocked N-terminus was dissolved in 25 μ l of 18 mM sodium phosphate buffer, pH 7.2, and digested with 0.1 unit of acyl amino acid-releasing enzyme for 6 h at 37°C. The digest was separated on the octadecylsilane column as described above.

Hydrazinolysis—The carboxyl-terminal amino acid of the protein was determined by vapor-phase hydrazinolysis according to Yamamoto *et al.* (9).

Amino Acid Composition and Sequence Analyses—Protein and peptide samples (0.5–3 nmol) were hydrolyzed with 5.7 M HCl for 22 h at 110°C under vacuum, and analyzed for amino acid contents using a Hitachi 835 amino acid analyzer. Tryptophan was determined after hydrolysis with 5.7 M HCl containing 4% mercaptoacetic acid (10). Destruction of S-carboxymethylcysteine was prevented by addition of 2-mercaptoethanol (0.5%) and extensive deaeration. Cyst(e)ine was also determined as cysteic acid after performic acid oxidation (11) using an amino acid analyzer modified for separation of strongly acidic amino acids (12). Amino acid sequences of the peptides (0.2–0.5 nmol) were determined on protein sequencers, model 470A and 473A (Applied Biosystems).

Determination of Disulfide Bond of FABP-2—Sea bass protein (16 nmol) was alkylated with iodoacetamide in 6 M guanidine-HCl, 0.1 M phosphate buffer, pH 7.0, and 5 mM EDTA with and without reduction with dithiothreitol. After removal of the reagents by ultrafiltration, the protein samples were digested with 5 μ g of lysyl endopeptidase in 2 M guanidine-HCl, 33 mM phosphate buffer, pH 7.0, and 1.7 mM EDTA for 3 h. The digests were separated on an octadecylsilane column (Capcell Pak C18, 4.6 \times 150 mm) equilibrated with 1% acetonitrile in 0.5% trifluoroacetic acid. Peptides differing between the two digests were analyzed for amino acid sequence.

Determination of Ligand-Binding Activity—Protein samples were defatted by slowly passing them through a column (0.9 \times 10 cm, 37°C) of Lipidex 1000 (13) equilibrated with 50 mM phosphate buffer, pH 7.0, and 1 mM EDTA. The protein peak was collected and quantified by amino acid analysis. The defatted protein (0.8 μ M in 50 mM phosphate buffer, 1 mM EDTA) was titrated with a fluorescent analog of fatty acid, DAUDA, dissolved in ethanol (14), and with a natural fluorescent fatty acid, *cis*-parinaric acid, in dimethylformamide (15) at 25°C. The concentrations of

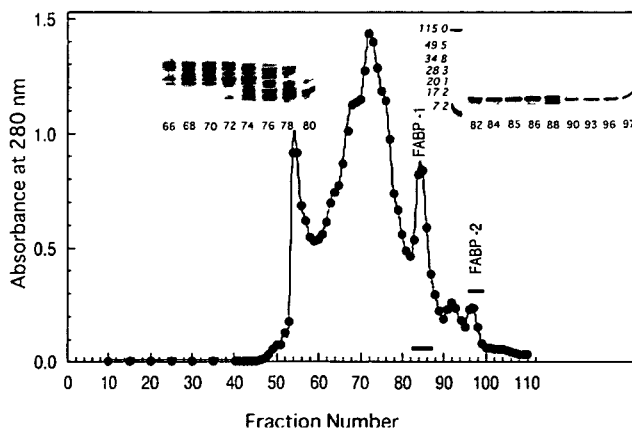


Fig. 1. Gel filtration of sea bass liver FABPs. Sephadex G-75 fractions containing low-molecular-mass proteins were pooled and chromatographed on a Sephacryl S-100 column (3 \times 100 cm) equilibrated with 30 mM Tris-HCl, pH 8.6, 1 mM EDTA. SDS-PAGE patterns of the aliquots from fractions (3 ml) are also shown. Numbers below the lanes are fraction numbers, and those beside the marker proteins are molecular mass in kDa. Every fraction containing low-molecular-mass proteins was examined for protein profile by HPLC on an octylsilane column (Capcell Pak C8, 4.6 \times 150 mm). Fractions containing pure proteins were pooled as indicated by short bars (FABP-1 and FABP-2).

Fig. 2. Titration curves for the binding of DAUDA and *cis*-parinaric acid to FABP-1 and FABP-2 of sea bass liver. The defatted proteins (0.8 μM in 50 mM phosphate buffer, 1 mM EDTA) were titrated with DAUDA (left) and *cis*-parinaric acid (right) at 25°C. Change in fluorescence intensity was recorded at 550 nm (DAUDA, excitation at 335 nm) or 415 nm (*cis*-parinaric acid, excitation at 310 nm) upon addition of increasing concentrations of the ligands. Open circles, FABP-1; filled circles, FABP-2. The solid lines are the theoretical curves for complex formation with DAUDA with dissociation constants $K_d = 0.51 \mu\text{M}$ (FABP-1) and $K_d = 3.3 \mu\text{M}$ (FABP-2). Those for binding of *cis*-parinaric acid are 0.09 μM (FABP-1) and 0.62 μM (FABP-2), respectively.

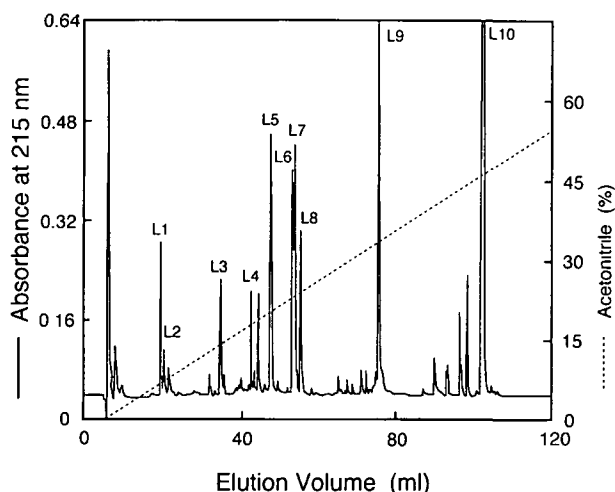
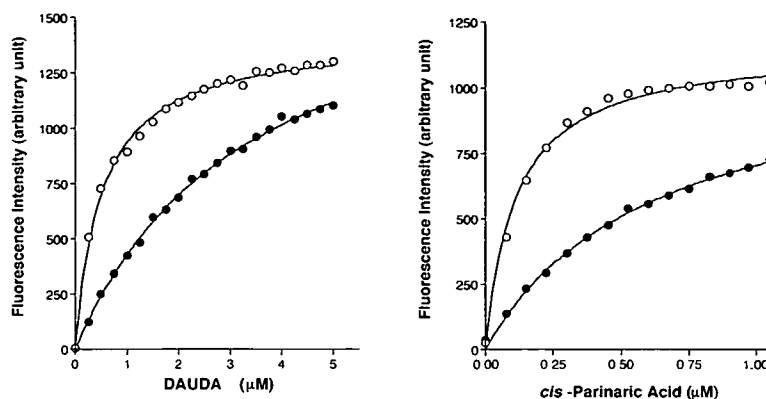


Fig. 3. Separation of lysyl endopeptidase peptides of FABP-2 by reversed-phase HPLC. The enzymatic digest was separated on an octadecylsilane column (4.6 \times 250 mm, ODS-120T) equilibrated with 0.05% trifluoroacetic acid and eluted with linear gradients of acetonitrile concentration as shown by the dotted lines. The flow rate was 0.5 ml/min. Peptides were numbered in the order of elution with the prefix L.

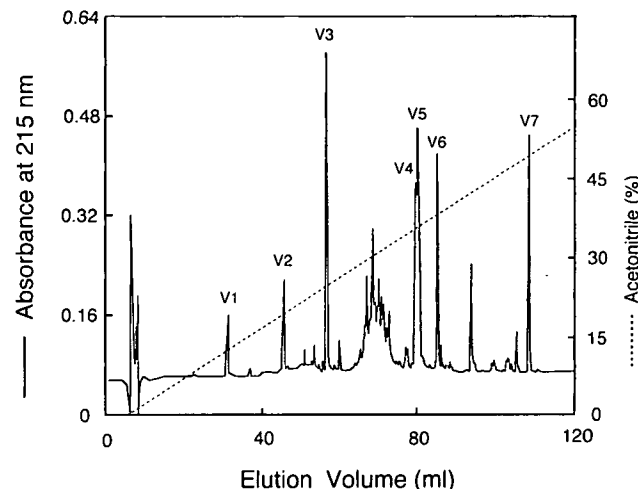


Fig. 4. Separation of *S. aureus* V8 protease peptides of FABP-2 by reversed phase HPLC. Reduced and alkylated protein was digested with *S. aureus* V8 protease, and the digest was separated as described in the legend to Fig. 3. Major peptides were numbered in the order of elution with the prefix V. V3 contained two peptides, V3a and V3b, which were separated by HPLC in 10 mM ammonium formate pH 4.5 instead of 0.05% trifluoroacetic acid.

DAUDA and *cis*-parinaric acid were determined by measuring the absorbance of the methanol solutions using molar extinction coefficients of 4,800 at 335 nm and 76,000 at 303 nm, respectively (16). The fluorescence intensity at 550 nm (excitation at 335 nm, DAUDA) or at 415 nm (excitation at 310 nm, *cis*-parinaric acid) was recorded with a Hitachi F-3010 spectrofluorometer. During a 30-s equilibration of the ligand and FABP, the shutter at the excitation side was closed to minimize photobleaching. The fluorescence intensity without protein was also measured at each fatty acid concentration and subtracted from the value for the protein sample. The concentration of FABP was determined by amino acid analysis after hydrolysis with 5.7 M HCl as described above. The results were fitted to a hyperbolic curve using the PRISM software (Graph Pad Software, San Diego) by non-linear regression.

Homology Modeling of Sea Bass and Zebrafish (*Danio rerio*) Liver FABPs—Three-dimensional models of sea bass FABP-2 and zebrafish liver FABP (17) were generated by the homology modeling method and optimized (18, 19) based upon the coordinates of mammalian FABPs (1EAL,

porcine ileum; 1LFO, rat liver; 1BWY, bovine heart; 1HMR and 1HMS, human muscle) in the Protein Data Bank (Research Collaboratory for Structural Bioinformatics). The coordinates for a theoretical shark liver FABP (accession code; P80049_C00002) were retrieved from the 3DCrunch, a large-scale comparative protein modeling project which automatically calculates three-dimensional models from all protein sequence entries of the SWISS-PROT and TrEMBL databases (20). Structures were visualized by the WebLab Viewer software (Molecular Simulations, San Diego).

Construction of a Phylogenetic Tree—The amino acid sequence of sea bass liver FABP-2 was aligned with those of mammalian and fish FABPs using the CLUSTAL W program of Thompson *et al.* (21). A phylogenetic tree was constructed by the neighbor-joining method (22) and visualized by the TreeView software (23).

RESULTS AND DISCUSSION

Purification and Characterization of Sea Bass Liver FABPs—Because of a large amount of the cytosolic pro-

teins, no distinct protein peaks were observed during gel filtration on Sephadex G-75 (not shown). Chromatographic fractions were examined for FABP by SDS-PAGE, and the eluant from 720 ml to 882 ml (fractions 43 through 50) was condensed by ultrafiltration and subjected to gel filtration on Sephacryl S-100 (Fig. 1). The low-molecular-mass pro-

teins were detected by SDS-PAGE in the three peaks eluted around 243–300 ml (fraction 82 through 100). Aliquots from fractions of these peaks were subjected to HPLC on an octylsilane column, and fractions showing essentially a single protein peak were combined. The first and third peaks contained essentially pure proteins, while rather

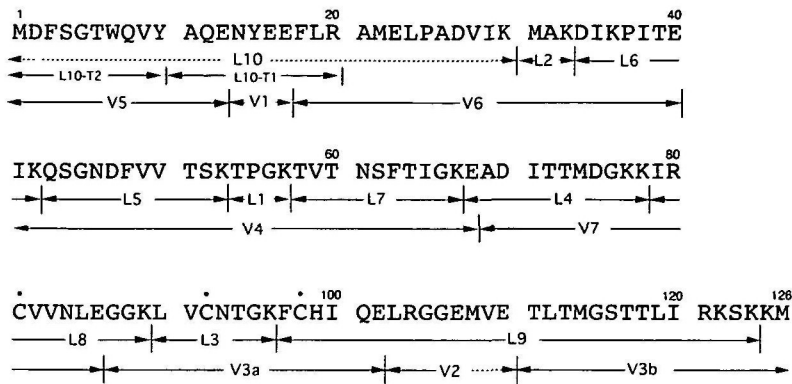


Fig. 5. Summary of the sequence analysis of sea bass FABP-2. Peptide regions where amino acid sequences were determined by the sequenator are indicated by solid lines. Those shown by dotted lines were not actually sequenced but confirmed by the amino acid compositions of the peptides. L and V represent lysyl endopeptidase peptides and *S. aureus* V8 protease peptides, respectively. The amino-terminus is blocked, probably by acetylation. The positions of the three cysteine residues are marked with dots.

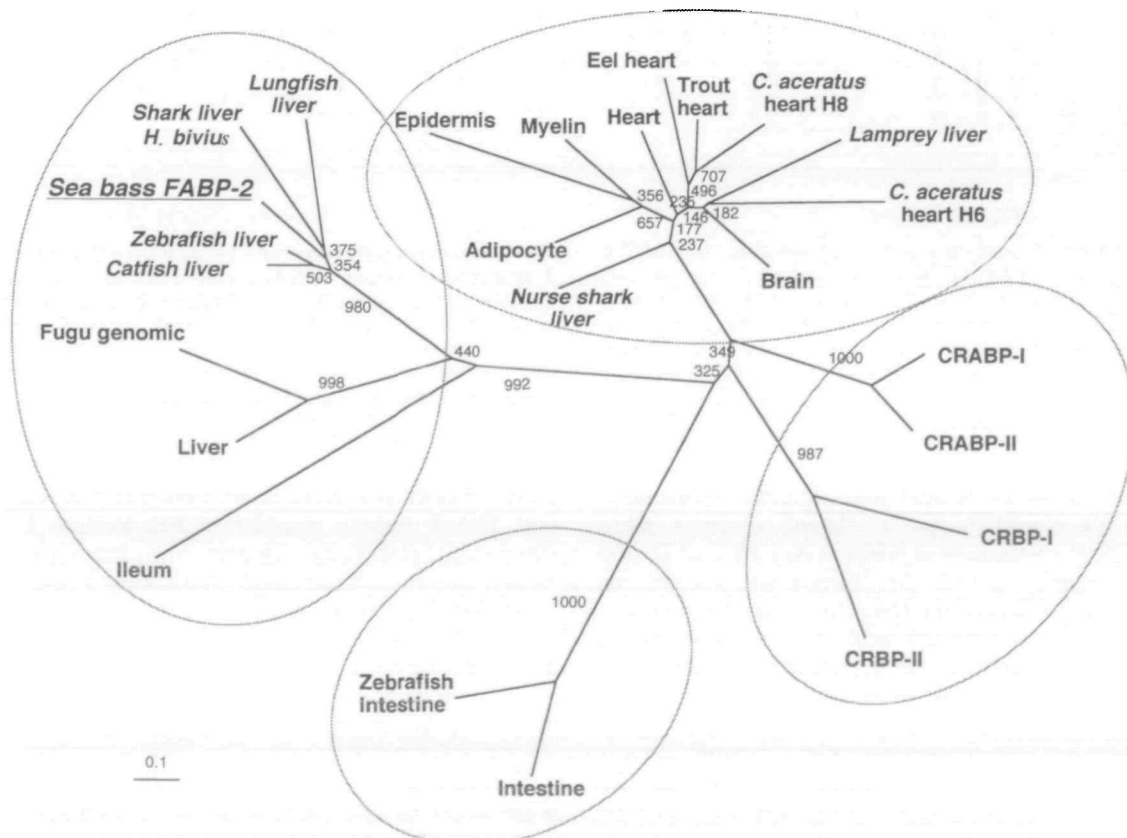


Fig. 6. Phylogenetic relationship of sea bass FABP-2 to other fish FABPs and tissue-specific FABPs of mammalia. Amino acid sequences of sea bass FABP-2 and principal FABPs of the vertebrate origins were aligned by CLUSTAL W (21). The unrooted tree was constructed by the neighbor-joining method (22) and displayed by Tree-View (23). Values for 1,000 bootstrap replications (21) are shown. Tissue-specific mammalian FABPs are human proteins except for the testis protein (mouse). The fish FABPs found in the liver are italicized. CRBP, cellular retinol-binding protein. CRABP, cellular retinoic

acid-binding protein. Sequences were retrieved from the Swiss-Prot (sp) and EMBL (emb) databases. *C. aceratus*, *Chaenocephalus aceratus* (Antarctic teleost fish, emb: U92442, heart H6, and U92448, heart H8); Eel, *Anguilla japonica* (emb: AB03966); Fugu, *Fugu rubripes* (emb: U90880); *H. biviuis*, *Halaelurus biviuis* (sp: P81653); Lungfish, *Lepidosiren paradoxus* (sp: P82289); Nurse shark, *Ginglymostoma cirratum* (sp: P80049); Zebrafish, *Danio rerio* (emb: AF254642, liver, and AF121346, intestine).

complex elution profiles were obtained for the second peak fractions by HPLC and no further investigation was made for the second peak. These two proteins, designated FABP-1 and FABP-2, differed in elution position on HPLC and amino acid compositions (not shown). It is remarkable that the two proteins with similar molecular masses were completely separated by gel filtration on Sephacryl S-100. It may be possible that FABP-1 exists as a dimer in solution, since concentration-dependent polymerization has been reported for rat heart FABP (24, 25).

Fatty Acid-Binding Activity—Figure 2 shows titration curves of FABP-1 and FABP-2 with DAUDA and *cis*-parinaric acid.

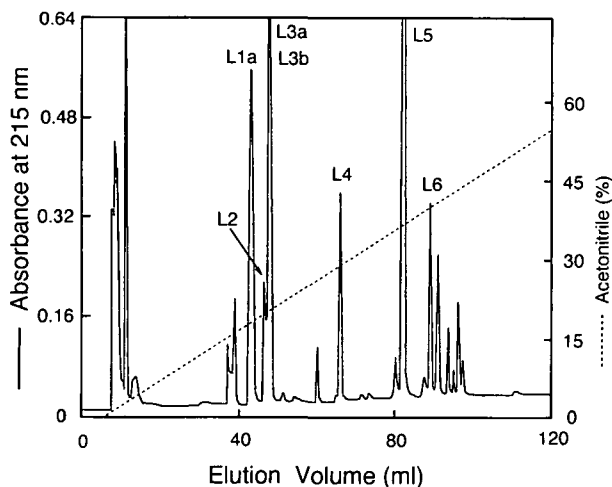


Fig. 7. Separation of lysyl endopeptidase peptides of FABP-1 by reversed-phase HPLC. The enzymatic digest was separated on an octadecylsilane column (4.6 × 250 mm, ODS-120T) equilibrated with 0.05% trifluoroacetic acid and eluted with linear gradients of acetonitrile concentration as shown by the dotted lines. The flow rate was 0.5 ml/min. Peptides used for sequence analysis were numbered in the order of elution with the prefix L. Peptides further purified by HPLC in 10 mM ammonium formate, pH 4.5, are indicated by the suffixes a and b. L5 had a blocked N-terminus and probably derived from the N-terminal region of FABP-1.

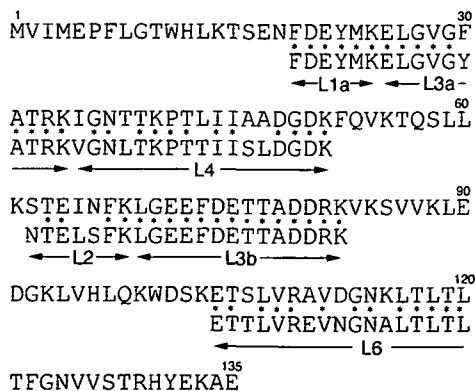


Fig. 8. Amino acid sequences of lysyl endopeptidase peptides of sea bass liver FABP-1 and comparison with the sequence of eel heart FABP. Six selected peptides were sequenced, and their homologous proteins were sought by use of the FASTA program (26). The sequences match best with those of cardiac FABPs of fish and mammalian brain FABPs. An alignment with eel (*Anguilla japonica*) heart FABP (EMBL: AB039666) is shown.

naric acid. Dissociation constants (K_d) for the binding of DAUDA and *cis*-parinaric acid are 0.5 and 0.09 μM for FABP-1, and 3 and 0.6 μM for FABP-2, respectively. The affinity of FABP-2 for DAUDA and *cis*-parinaric acid is rather low as compared with other FABPs (14, 15). This protein may have a higher affinity for some other compounds.

Primary Structure of Sea Bass Liver FABP-2—Direct sequence analysis of sea bass liver FABP-2 failed to detect the N-terminal sequence due to the blocked terminus. The C-terminal residue was supposed to be methionine by vapor phase hydrazinolysis, which yielded 0.1 mol methionine per mol protein. Figure 3 shows the elution profile of the lysyl endopeptidase digest of FABP-2 on the octadecylsilane column. Prior to sequence analysis, amino acid compositions of these peptides had been analyzed (data not shown). All peptides except for L10 were sequenced to their C-termini. The sequence of a rather long peptide, L9, was confirmed by analyzing its cyanogen bromide subpeptides. L10 had a blocked N-terminus and this was digested with trypsin. Two tryptic peptides L10-T1 and L10-T2 were recovered. T2 was digested with acylamino acid releasing enzyme (Takara), the digest was separated on an octadecylsilane column and the deblocked peptide was fully sequenced. An additional small peak eluted by 12% acetonitrile.

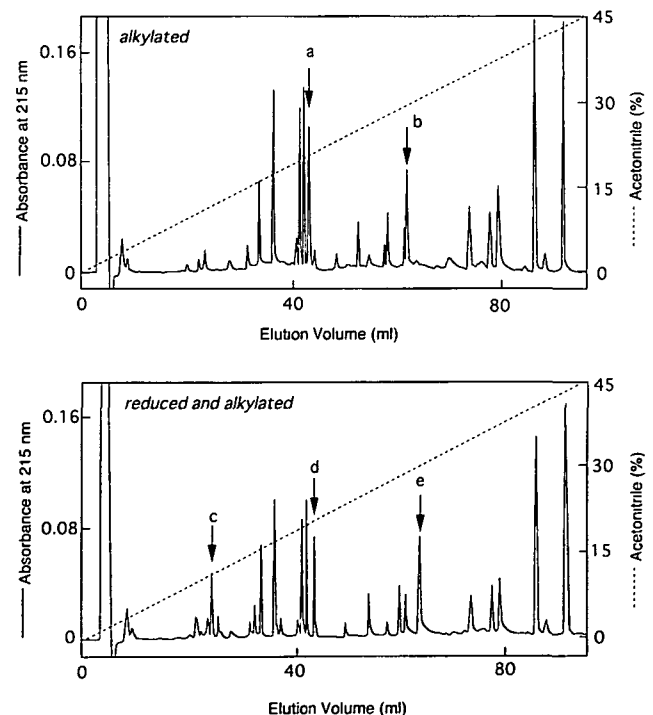


Fig. 9. Comparison of peptide maps of FABP-2 before (upper panel) and after (lower panel) reduction. Sea bass protein (16 nmol) was alkylated with iodoacetamide in 6 M guanidine-HCl, 0.1 M phosphate buffer, pH 7.0, and 5 mM EDTA with and without reduction with dithiothreitol. The protein samples were digested with lysyl endopeptidase in 2 M guanidine-HCl, 33 mM phosphate buffer, pH 7.0, and 1.7 mM EDTA for 3 h. The digests were separated on an octadecylsilane column (Capcell Pak C18, 4.6 × 150 mm, Shiseido) equilibrated with 1% acetonitrile in 0.5% trifluoroacetic acid. Peptides marked a–e were found to be derived from cyst(e)ine-containing regions of FABP-2.

trile was hydrolyzed and methionine was identified, confirming the N-terminus as a blocked methionine residue, probably acetylmethionine, which was consistent with the composition data for the peptide. The remainder of L10 was sequenced by analyzing L10-T1, and V1 and V6 of *S. aureus* V8 peptides described below. The lysyl endopeptidase peptides were aligned by the analysis of overlapping peptides obtained by *S. aureus* V8 protease digestion (Fig. 4). The sequence analysis is summarized in Fig. 5.

Phylogenetic Analysis of Sea Bass FABP-2—A molecular phylogenetic tree was constructed by a CLUSTAL W alignment of sea bass FABP-2 and other fish liver FABPs with the fourteen mammalian FABP subtypes (Fig. 6). In accordance with the previous reports (1, 2, 4), the tree has four major branches corresponding to the four FABP subfamilies, of which sea bass FABP-2 is placed in the hepatic FABP subfamily.

Partial Structure of Sea Bass Liver FABP-1—This protein also had a blocked N-terminus and was digested with lysyl endopeptidase. The peptides were separated by HPLC (Fig. 7) and partial amino acid sequences of six selected peptides were determined as shown in Fig. 8. They are aligned with the most similar eel FABP detected by the

FASTA program (26). FABP-1 is a close homologue of Japanese eel (*Anguilla japonica*) heart FABP (EMBL: AB038695), which is a member of the cardiac FABP subfamily. In contrast to the expression of a single hepatic FABP in the mammalian livers, the fish livers appear to contain multiple FABPs of different subtypes (5, 6, 27). It is known that livers of fishes are more adipocyte-like, and, in some species, function as a source of buoyancy generated by large amounts of neutral lipids (28). Use of wax esters instead of triglycerides as a major storage form of lipid is frequently observed in fish liver and adipose tissue (28). The presence of two types of FABP may reflect this unique lipid metabolism in fish and could be a clue to understand the functional diversity of FABP subfamilies.

Disulfide Bond in FABP-2—First, the state of the three half-cystine residues in FABP-2 was examined by amino acid analysis. Performic acid oxidation yielded 3.0 mol of cysteic acid per mol protein, while alkylation in the denaturant gave 1.1 mol of *S*-carboxymethylcysteine per mol protein. The results indicate that only one of the three half-cysteine residues has a free thiol group, and that the other two may form a disulfide bond. Figure 9 shows comparative peptide maps of the alkylated and the reduced and alky-

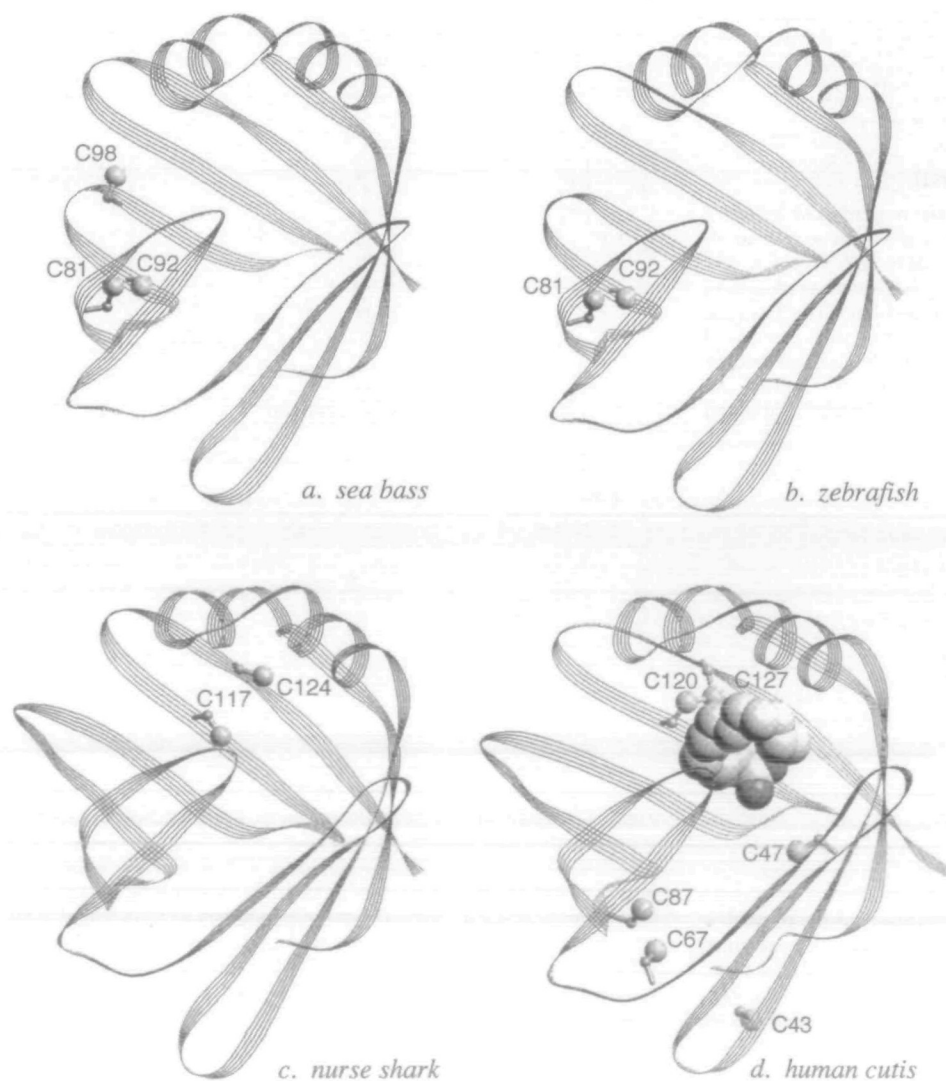


Fig. 10. Three-dimensional models of (a) sea bass liver FABP-2, (b) zebrafish liver FABP, (c) nurse shark liver FABP, and (d) human cutaneous FABP. Models were generated by the comparative modeling method (18, 19) and figures were drawn by the WebLab Viewer (Molecular Simulations). The coordinates for the recombinant human cutaneous FABP with bound palmitate (1B56.pdb) were obtained from the Protein Data Bank at the Research Collaboratory for Structural Bioinformatics. Sulfur atoms of cysteine residues are shown by spheres of an arbitrary dimension. Palmitate in the recombinant human cutaneous FABP is shown by the space-filling model.

lated FABP-2 digested with lysyl endopeptidase. Although some minor differences are seen in the maps, the major difference is the absence of peptide a of alkylated protein and the appearance of two additional peptides (peptides c and d) in the reduced and alkylated protein. When peptide a was sequenced, two sequences which could be interpreted to be LVXNTG- and IRXVVN- were simultaneously detected. From peptide c and peptide d, sequences LVCNT- and IRCVV- were obtained (C: identified as S-carbamoylmethylcysteine), which corresponded to the N-terminal sequences of L3 and L8, respectively, in Fig. 5. Peptides b and e both gave the same sequence as that of L9 in Fig. 5 (FCHIQEL, C: S-carbamoylmethylcysteine). These results indicate that FABP-2 contains one disulfide bond between Cys-81 and Cys-92, and that Cys-98 is free cysteine.

A three-dimensional model of sea bass FABP-2 generated by the comparative modeling method (18, 19) is shown in Fig. 10. The predicted structure is similar to those of typical FABPs consisting of two orthogonal β -sheets and two α -helices connected by a short peptide (Fig. 10a). It is seen that Cys-81 and Cys-92 are present in the close proximity, with their side chain S γ atoms being only 4 Å apart, while the side chain of Cys-98 is oriented in the opposite direction to these cysteine residues and its S γ is 8.5 and 10.5 Å distant from those of the other cysteines. This model supports the presence of a disulfide bond between Cys-81 and Cys-92. Figure 10b shows a three-dimensional model of a recently reported zebrafish liver FABP, which also has two spatially close cysteine residues. Mass spectrometric data of an enzymatic peptide of nurse shark (*G. cirratum*) liver FABP appears to indicate a disulfide bond (3), which is also supported by the theoretical model (Fig. 10c). In a rat cutaneous FABP preparation, we have identified two disulfide bonds (7), one of which was seen in the crystal structure of a recombinant human cutaneous FABP expressed in *Escherichia coli* (29) as shown in Fig. 10d. These two FABPs belongs to the cardiac FABP subfamily, and the positions of the disulfide bonds are different from those of the sea bass and zebrafish proteins. Disulfide bonds in cutaneous FABP appear not to be directly involved in ligand-binding activity, since recombinant rat and mouse proteins with no disulfide bonds have fatty acid-binding activity (7, 30). Similarly, the disulfide bond in sea bass FABP-2 may not be critical for the ligand-binding activity, since there was no difference when the DAUDA-binding assay was carried out in the presence or absence of 10 mM dithiothreitol (data not shown). However, the presence of disulfide bonds in FABPs and evolutionary conservation of spatially close cysteine pairs in FABPs among distant species suggests a potential regulatory mechanism by thiol-disulfide interchange reaction, since the function of FABPs is not confined to that of mere transporters of fatty acids. They are now shown to be involved in regulation of many cellular processes such as cell differentiation and growth (31, 32), repair of the peripheral nerve system (33), protein biosynthesis (34), and induction of cancer metastasis (35), some of which might be under the redox regulation. Oxidative formation and reductive cleavage of disulfide bonds of cellular proteins have long been implicated in regulatory mechanisms of protein functions (36). Recently, disulfide bond formation in the stress proteins has been established as a key step in the response to oxidative stress (37). Disulfide bond formation is important for dimerization of tran-

scription factors to bind to DNA (38, 39), and regulation of enzyme activities such as human protein phosphotyrosine phosphatase and plant glycolytic enzymes is also disulfide-mediated (40, 41). Electrophoretic and chemical evidence indicates the presence of dimeric species of human cardiac muscle FABP linked by a disulfide bond (42). It is tempting to speculate that these intra- and inter-molecular disulfide bonds may be regulating functions of FABP.

S. O. thanks Dr. Tokuji Ikenaka, professor emeritus of Osaka University, for his encouragement.

REFERENCES

- Schleicher, C.H., Córdoba, O.L., Santomé, J.A., and Dell'Angelica, E.C. (1995) Molecular evolution of the multigene family of intracellular lipid-binding proteins. *Biochem. Mol. Biol. Int.* **36**, 1117–1125
- Baba, K., Abe, K.T., Tsunasawa, S., and Odani, S. (1999) Characterization and primary structure of a fatty acid-binding protein and its isoforms from the liver of the amphibia, *Rana catesbeiana*. *J. Biochem.* **125**, 115–122
- Medzihradzsky, K.F., Gibson, B.W., Kaur, S., Yu, Z., Medzihradzsky, D., Burlingame, A.L., and Bass, N.M. (1992) The primary structure of fatty-acid-binding protein from nurse shark liver. Structural and evolutionary relationship to the mammalian fatty-acid-binding protein family. *Eur. J. Biochem.* **203**, 327–339
- Baba, K., Takahashi, Y., Aoyagi, Y., and Odani, S. (1999) The amino acid sequence of a lamprey (*Entosphenus japonicus*) liver fatty acid-binding protein identified its close relationship to cardiac fatty acid-binding proteins of Mammalia. *Comp. Biochem. Physiol. B. Biochem. Mol. Biol.* **123**, 223–228
- Córdoba, O.L., Sanchez, E.I., and Santomé, J.A. (1999) The main fatty acid-binding protein in the liver of the shark (*Halaeutonus bivius*) belongs to the liver basic type. Isolation, amino acid sequence determination and characterization. *Eur. J. Biochem.* **265**, 832–838
- Córdoba, O.L., Sanchez, E.I., Veerkamp, J.H., and Santomé, J.A. (1998) Presence of intestinal, liver and heart/adipocyte fatty-acid-binding protein types in the liver of a chimaera fish. *Int. J. Biochem. Cell. Biol.* **30**, 1403–1413
- Odani, S., Namba, Y., Ishii, A., Ono, T., and Fujii, H. (2000) Disulfide bonds in rat cutaneous fatty acid-binding protein. *J. Biochem.* **128**, 355–361
- Sakiyama, F. and Masaki, T. (1994) Lysyl endopeptidase of *Achromobacter lyticus*. *Methods Enzymol.* **244**, 126–137
- Yamamoto, A., Toda, H., and Sakiyama, F. (1989) Vapor-phase hydrazinolysis for microdetermination of carboxyl-terminal amino acids of proteins. *J. Biochem.* **106**, 552–554
- Matsubara, H. and Sasaki, R.M. (1969) High recovery of tryptophan from acid hydrolysates of proteins. *Biochem. Biophys. Res. Commun.* **35**, 175–181
- Hirs, C.H.W. (1967) Performic acid oxidation. *Methods Enzymol.* **11**, 59–62
- Odani, S., Koide, T., Ono, T., and Aoyagi, Y. (1988) Analysis of strongly acidic amino acids by the conventional amino acid analyzer: Application to analysis of protein-bound glutathione and cysteine. *Anal. Biochem.* **171**, 305–309
- Glatz, J.F.C. and Veerkamp, J.H. (1983) A radiochemical procedure for the assay of fatty acid binding protein. *Anal. Biochem.* **132**, 89–95
- Thumser, A.E.A., Voysey, J., and Wilton, D.C. (1996) Mutations of recombinant rat liver fatty acid-binding protein at residues 102 and 122 alter its structural integrity and affinity for physiological ligands. *Biochem. J.* **314**, 943–949
- Nemecz, G., Hubbell, T., Jeferson, J.R., Lowe, J.B., and Schroeder, F. (1991) Interaction of fatty acids with recombinant rat intestinal and liver fatty acid-binding proteins. *Arch. Biochem. Biophys.* **286**, 300–309
- Haugland, R.H. (1996) Fluorescent phospholipids, fatty acids

- and sterols in *Handbook of Fluorescent Probes and Research Chemicals* (Spence, M.T.Z., ed.) pp. 287–308, Molecular Probes, Eugene
17. Denovan-Wright, E.M., Pierce, M., Sharma, M.K., and Wright, J.M. (2000) cDNA sequence and tissue-specific expression of a basic liver-type fatty acid binding protein in adult zebrafish (*Danio rerio*). *Biochim. Biophys. Acta* **1492**, 227–232
 18. Guex, N. and Peitsch, M.C. (1997) SWISS-MODEL and the Swiss-PdbViewer: An environment for comparative protein modelling. *Electrophoresis* **18**, 2714–2723
 19. Peitsch, M.C. (1996) ProMod and Swiss-Model: Internet-based tools for automated comparative protein modelling. *Biochem. Soc. Trans.* **24**, 274–279
 20. Peitsch, M.C., Wilkins, M.R., Tonella, L., Sanchez, J.-C., Appel, R.D., and Hochstrasser, D.F. (1997) Large scale protein modelling and integration with the SWISS-PROT and SWISS-2DPAGE databases: the example of *Escherichia coli*. *Electrophoresis* **18**, 498–501
 21. Thompson, J.B., Higgins, D.G., and Gibson, T.J. (1994) CLUSTAL W: improving the sensitivity of progressive multiple sequence alignment through sequence weighting, position-specific gap penalties and weight matrix choice. *Nucleic Acids Res.* **22**, 4673–4680
 22. Saitou, N. and Nei, M. (1987) The neighbor-joining method: a new method for reconstructing phylogenetic trees. *Mol. Biol. Evol.* **4**, 406–425
 23. Page, R.D. (1996) TreeView: an application to display phylogenetic trees on personal computers. *Comput. Appl. Biosci.* **12**, 357–358
 24. Fournier, N.C. and Rahim, M. (1985) Control of energy production in the heart: a new function for fatty acid binding protein. *Biochemistry* **24**, 2387–2396
 25. Fournier, N.C. and Rahim, M. (1990) Role of fatty acid-binding protein in cardiac fatty acid oxidation. *Mol. Cell. Biochem.* **98**, 149–159
 26. Pearson, W.R. (1990) Rapid and sensitive sequence comparison with FASTP and FASTA. *Methods Enzymol.* **183**, 63–98
 27. De Pietro, S.M. and Santome, J.A. (1996) Presence of two new fatty acid binding proteins in catfish liver. *Biochem. Cell. Biol.* **74**, 675–680
 28. Love, R.M. (1970) *The Chemical Biology of Fishes*, Academic Press, London, 1970
 29. Hohoff, C., Borchers, T., Rustow, B., Spener, F., and van Tilbeurgh, H. (1999) Expression, purification, and crystal structure determination of recombinant human epidermal-type fatty acid binding protein. *Biochemistry* **38**, 12229–12239
 30. Kane, C.D., Coe, N.R., Vanlandingham, B., Krieg, P., and Bernlohr, D.A. (1996) Expression, purification, and ligand-binding analysis of recombinant keratinocyte lipid-binding protein (MAL-1), an intracellular lipid-binding protein found overexpressed in neoplastic skin cells. *Biochemistry* **35**, 2894–2900
 31. Borchers, T., Hohoff, C., Buhlmann, C., and Spener, F. (1997) Heart-type fatty acid binding protein— involvement in growth inhibition and differentiation. *Prostaglandins Leukot. Essent. Fatty Acids* **57**, 77–84
 32. Sorof, S. (1994) Modulation of mitogenesis by liver fatty acid binding protein. *Cancer Metastasis Rev.* **13**, 317–336
 33. De Leon, M., Welcher, A.A., Nahin, R.H., Liu, Y., Ruda, M.A., Shooter, E.M., and Molina, C.A. (1996) Fatty acid binding protein is induced in neurons of the dorsal root ganglia after peripheral nerve injury. *J. Neurosci. Res.* **44**, 283–292
 34. Zimmerman, A.W. and Veerkamp, J.H. (1998) Members of the fatty acid-binding protein family inhibit cell-free protein synthesis. *FEBS Lett.* **437**, 183–186
 35. Jing, C., Beesley, C., Foster, C.S., Rudland, P.S., Fujii, H., Ono, T., Chen, H., Smith, P.H., and Ke, Y. (2000) Identification of the messenger RNA for human cutaneous fatty acid-binding protein as a metastasis inducer. *Cancer Res.* **60**, 2390–2398
 36. Gilbert, H.F. (1990) Molecular and cellular aspects of thiol-disulfide exchange. *Adv. Enzymol. Relat. Areas Mol. Biol.* **63**, 69–172
 37. Jakob, U., Muse, W., Eser, M., and Bardwell, J.C.A. (1999) Chaperone activity with a redox switch. *Cell* **96**, 341–352
 38. Markus, M. and Benezra, R. (1999) Two isoforms of protein disulfide isomerase alter the dimerization status of E2A proteins by a redox mechanism. *J. Biol. Chem.* **274**, 1040–1049
 39. Shao, D., Creasy, C.L., and Bergman, L.W. (1998) A cysteine residue in helixII of the bHLH domain is essential for homodimerization of the yeast transcription factor Pho4p. *Nucleic Acids Res.* **26**, 710–714
 40. Caselli, A., Marzocchini, R., Camici, G., Manao, G., Moneti, G., Pieraccini, G., and Ramponi, G. (1998) The inactivation mechanism of low molecular weight phosphotyrosine-protein phosphatase by H₂O₂. *J. Biol. Chem.* **273**, 32554–32560
 41. Anderson, L.E., Li, D., Prakash, N., and Stevens, F.J. (1995) Identification of potential redox-sensitive cysteines in cytosolic forms of fructosebisphosphatase and glyceraldehyde-3-phosphate dehydrogenase. *Planta* **196**, 118–124
 42. Nielsen, S.U., Vorum, H., Spener, F., and Brodersen, R. (1990) Two-dimensional electrophoresis of the fatty acid binding protein from human heart: evidence for a thiol group which can form an intermolecular disulfide bond. *Electrophoresis* **11**, 870–877